On Detection of Anomalous VHF Propagation over the Adriatic Sea Utilising a Software-Defined Automatic Identification System Receiver

Valčić, Sanjin; Brčić, David

Journal of
Marine Science and Engineering

MDPI

Communication

On Detection of Anomalous VHF Propagation over the Adriatic Sea Utilising a Software-Defined Automatic Identification System Receiver

Sanjin Valčić [1,2,*] and David Brčić [1]

[1] Faculty of Maritime Studies, University of Rijeka, 51000 Rijeka, Croatia; david.brcic@pfri.uniri.hr
[2] Centre for Marine Technologies, Faculty of Maritime Studies, University of Rijeka, 51000 Rijeka, Croatia
* Correspondence: sanjin.valcic@pfri.uniri.hr

Abstract: This paper represents observations on detection of Very High Frequency (VHF) anomalous propagation over the area of the Adriatic Sea. During the research campaign, a Software Defined Radio (SDR) Automatic Identification System (AIS) receiver was employed for collection of AIS data packets at a fixed location in the Northern Adriatic. Data were collected during the 24-h period (25 February 2023 15:32 LT to 26 February 2023 15:32 LT), providing information from 115 AIS targets, or 159 965 AIS packets with 54.3% Packet Error Rate (PER), respectively. Subsequent analysis and post-processing of successfully demodulated signals and decoded packets was presented further. In certain instances, the SDR AIS receiver detected, received and decoded data packets from AIS targets distant several orders of magnitude larger than the VHF nominal ranges. To determine the magnitude of line-of-sight and over-the-horizon radio waves propagation, the great circle distances between the SDR AIS receiver antenna and AIS packets' decoded positions were calculated, revealing hundreds of Nautical Miles (NM). Possible reasons for these occurrences, including tropospheric scattering, diffraction, ionospheric sporadic E layer and refraction were discussed and evaluated, in accordance, among others, with the previous research. By exclusion criteria and neglection of possible causes, it was concluded that the enhanced, over-the-horizon propagation of AIS signals occurred as a result of refraction effects, namely trapping/ducting, subrefraction and superrefraction. Data from nine World Meteorological Organization (WMO) radiosondes surrounding the greater reception area were collected for the same observation periods. Atmospheric profiles were created using Advanced Refractive Effects Prediction System (AREPS) program, and analysed for each individual station measurement. The results confirmed anomalous, over-the-horizon enhanced propagation and their probable origins, i.e., the occurrence of refractive conditions in the atmosphere over the Adriatic Sea area. These findings provide a solid foundation for further research in the area of propagation of VHF signals and their anomalous features caused by the atmospheric phenomenon effects.

Keywords: very high frequency; automatic identification system; software defined radio; anomalous propagation; over-the-horizon propagation

Citation: Valčić, S.; Brčić, D. On Detection of Anomalous VHF Propagation over the Adriatic Sea Utilising a Software-Defined Automatic Identification System Receiver. *J. Mar. Sci. Eng.* **2023**, *11*, 1170. https://doi.org/10.3390/jmse11061170

Academic Editor: Mihalis Golias

Received: 11 May 2023
Revised: 29 May 2023
Accepted: 30 May 2023
Published: 2 June 2023

1. Introduction

The maritime Automatic Identification System, is a digital communication system that serves for the automatic exchange of data between different AIS stations, using the Time Division Multiple Access (TDMA) schemes on two 25 kHz maritime VHF communication channels (161.975 MHz and 162.025 MHz). Its technical characteristics are defined and recommended by the International Telecommunication Union (ITU) [1]. On each channel, data is transmitted synchronously in packets within 2250 time slots of one-time frame (60 s) at a rate of 9600 bits per second (bps). Stations and devices that use AIS technology are shipborne Classes A and B, base stations, Aids to Navigation (AtoN), Search and Rescue (SAR) aircraft stations (airborne mobile equipment) and SAR devices: AIS-SART, EPIRB-AIS, MOB-AIS. The maritime AIS has been a very well-researched topic since the era before

its official introduction on ships and other stations. The authors in [2] analyzed possible problems in Self Organizing Time Division Multiple Access (SOTDMA) schemes, such as those used by the AIS, and emphasized how the so-called hidden users can cause the interference on the shared channel. Furthermore, the authors in [3] analyzed the technical characteristics and functionality of the system, providing an overview of its future potential applications, such as Vessel Traffic Service (VTS). A similar research and analysis were carried out in [4], in which the advantages and disadvantages of using the AIS in the United States' Maritime Domain Awareness (MDA) system were evaluated. The research conducted in [5] analysed the possibility of using the collected AIS data to avoid collisions in areas of heavy maritime traffic, while the authors in [6] pointed out the inconsistency of AIS data in the decision-making process during the collision avoidance. In [7,8], the methodologies for the extraction of traffic routes and the detection of their deviations based on raw AIS data were presented. Moreover, the authors in [9,10] made an exhaustive review of the literature in order to present the purposes for which AIS and its data are used, except for the safety of navigation. On the other hand, the authors in [11] analyzed the application of AIS to improve existing ship classification methods in synthetic aperture radar images.

The research presented in this paper focuses mainly on the reception of the VHF radio waves and processing of AIS data. In order to receive AIS data, i.e., data packets, it is necessary to have a suitable receiver with a demodulator and decoder. There are many commercial AIS receivers that cost from several hundred to several thousand US dollars. However, with the development of the Software Defined Radio (SDR), it is possible to produce and assemble low-cost AIS receivers. Namely, the SDR is a programmable radio system (tuner) for transmitting and/or receiving signals, in which processes such as modulation/demodulation or encoding/decoding are performed by the software [12,13]. Thus, the authors in [14] described the configuration of an AIS receiver based on a modular design using a receiver RX1 Radiometrix, a modem DV-MEGA and a microcontroller Arduino UNO R3. The author in [15] presented the design of the SDR AIS receiver for a satellite, while the authors in [16] created and tested a prototype of the SDR AIS, using ADALM-Pluto SDR and Matlab program. However, the aforementioned testing was based on the AIS signal strength, not demodulated and decoded AIS data. The authors in [17] had a similar approach and presented the concept of a software defined radio with a flexible RF front end, where the evaluation of the AIS receiver was made exclusively on its performance. Moreover, the authors in [18] have also assembled an SDR AIS receiver and only tested it based on the spectral analysis and comparison with a commercial AIS transceiver. In [19], the authors used the HackRF One SDR and the GNU Radio project and successfully tested the transmission and reception of AIS data packets and messages. Furthermore, the authors in [20] used the RTL-SDR based AIS receiver and their software written completely in C to demodulate the received AIS signals.

Regardless of which AIS receiver is used (hardware- or software-defined), the terrestrial range of AIS signal reception is limited by the spatial propagation of VHF radio waves, i.e., by the line-of-sight or the radio horizon in the standard atmosphere conditions. However, given the variable nature of Earth's atmosphere, it is not rare that AIS/VHF signals can be received and detected at great distances, i.e., over-the-horizon. Thus, the authors in [21] used experimental measurements to analyze the strength of the received VHF signals at distances greater than 200 miles. Furthermore, the authors in [22] analyzed big AIS data collected during 3 days by the United States Coast Guard (USCG). Based on the collected data, they detected 6677 signals from ships that were more than 1000 km away from coastal stations. In [23], the authors analyzed the received AIS signal from the over-the-horizon ship in the Yellow Sea area. The author in [24] modelled the impact of North Sea weather conditions on the performance of AIS and coastal radar systems and showed over-the-horizon propagation. By reviewing the aforementioned and additional literature on over-the-horizon AIS/VHF radio signal propagation, it can be stated that the conditions for such propagation could be radio waves' diffraction by the (sea) sur-

face, tropospheric scattering, ionospheric sporadic E layer and refraction (subrefraction, superrefraction, ducting) [22,25–27].

Prompted by all of the above, as well as by the fact that the comprehensive literature review did not reveal the use of SDR AIS receivers for the detection of anomalous propagation of VHF radio waves, the main hypothesis of this research is formulated as follows: By using a simple SDR AIS receiver, it is possible to detect anomalous propagation conditions of VHF radio waves, by analysing, evaluating and verifying the collected AIS data. Therefore, the main objective of the research presented in this paper was to assemble a simple SDR AIS receiver for collecting AIS data packets at a fixed location in the northern Adriatic area in order to (i) analyse its performance, and to (ii) eventually detect over-the-horizon AIS signals, i.e., AIS targets. An additional objective was to determine and prove the cause of the detected anomalous propagation of VHF radio waves.

The rest of the paper is organized as follows: In the Experimental setup and Methodology section, the equipment and its connection methods for assembling a simple SDR AIS receiver are described in detail. Additionally, it is presented how the built-in Matlab program is used to demodulate AIS signals and decode AIS data packets. In the Results Analysis and Discussion section, a detailed analysis, processing and verification of the collected AIS data is presented. Moreover, proving the cause of the detected anomalous propagation of VHF radio waves is also demonstrated and discussed.

2. Experimental Setup and Methodology

The equipment used to assemble the SDR AIS receiver is shown in Figure 1.

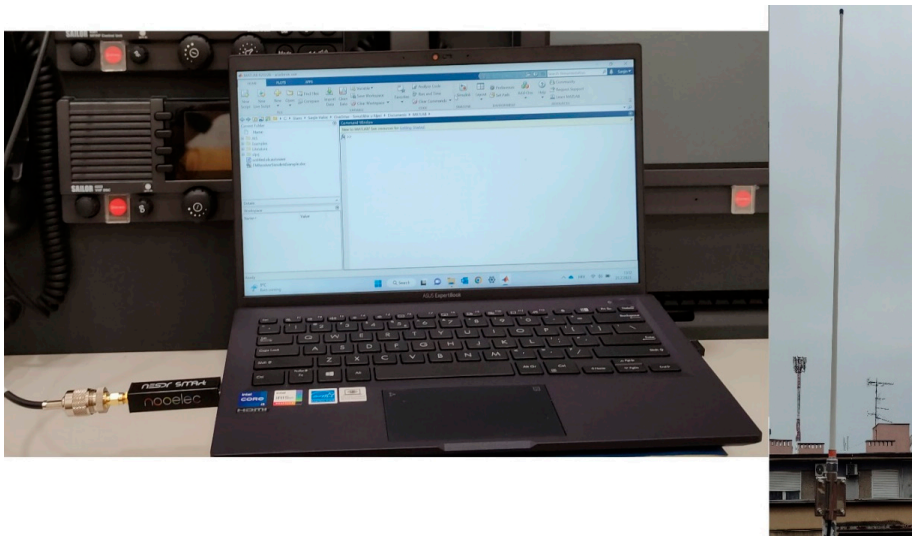

Figure 1. SDR AIS receiver.

The NESDR SMArt v5 is connected to a computer via a USB interface at the one end [28]. The computer has an Intel i5-1135g7 processor, 16 GB of RAM and a 64-bit operating system (Windows 11). The MathWorks MATLAB® R2022b, as well as Communications Toolbox™ and Communications Toolbox Support Package for RTL-SDR Radio, are installed on the specified operating system to control NESDR SMArt v5. The above software packages are required to run the built-in program Ship Tracking Using AIS Signals [29].

On the other end, the NESDR SMArt v5 is connected via a male SMA to SO-239 nickel-plated adapter to connect to a 40 m long RG 213/U coaxial cable, which is connected to a Marine VHF Glass Fiber Antenna (Scan Antenna VHF74). The mentioned antenna is a full half-wave dipole located at 45.3303 N, 14.436 E, 32 m AMSL and has the following characteristics [30]:

- 1.36 m length;
- 2.6 dBi gain;

- vertically polarized;
- VSWR < 1.6:1 in the frequency range from 156 to 162.5 MHz;
- characteristic impedance of 50 ohms.

In the previously mentioned built-in program, a reception time of 86,400 s (24 h) and a centre frequency of 162 MHz were set (given that the code uses a symbol rate of 9600 Hz and 24 samples per symbol, both AIS channels were scanned in this way). During the reception, successfully demodulated and decoded data were stored in a text file (data log) and displayed on the data viewer, i.e., on the graphical user interface (GUI). After the end of the reception (25 February 2023/15:32–26 February 2023/15:32), the subsequent processing and analysis of the decoded and displayed data followed.

3. Results Analysis and Discussion

During the 24-h period, the SDR AIS receiver detected 159,965 and decoded 73,090 AIS packets, which resulted in 54.3% Packet Error Rate (PER). Amongst these 73,090 successfully decoded AIS packets, data viewer showed 115 AIS targets. The list of decoded AIS targets within the data viewer is presented in Appendix A. Targets are displayed by their decoded Maritime Mobile Service Identity (MMSI) numbers, together with their decoded position (longitude and latitude) and the time of their last decoded AIS packet.

Further analysis of displayed positions showed that 4 AIS targets (#7, #79, #86 and #92) were decoded with an error (significantly deviated from other presented positions). Furthermore, all decoded and displayed AIS targets can be verified on the Marine Traffic Live Map [31]. By verifying the AIS target #7 (MMSI: 2383500, AIS base station), it can be concluded that its AIS packets were successfully decoded, but something went wrong with the AIS target itself, i.e., the base station (Figure 2).

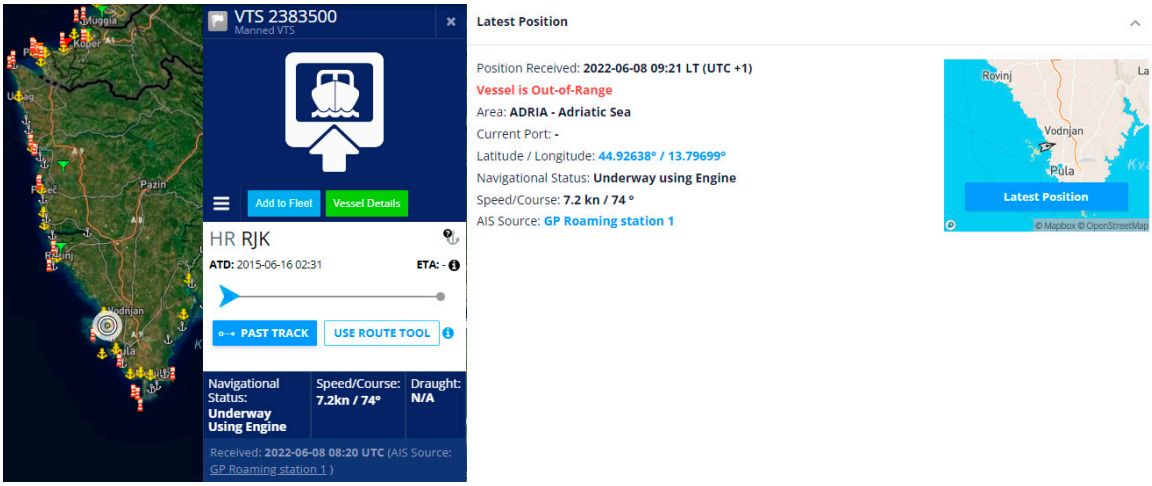

Figure 2. AIS target #7 [31].

Investigation into the data log of all successfully decoded AIS packets showed that 10,100 (out of 73,090 = 13.82%) were received from this AIS target, meaning that its data packets were received on average every 9 s. This can be related to the nominal reporting interval intended for AIS base stations (10 s) [11].

Analysing further, AIS packets from the AIS target #79 (MMSI: 0) were received and unsuccessfully decoded only 25 times (0.03%), meaning that 25 times Cyclic Redundancy Check (CRC) code was detected and decoded, but the AIS packet as a whole was erroneous and contained no data.

The AIS target #86 (MMSI: 743195360) was decoded and displayed only once, and therefore was neglected in this analysis. The same applies on the AIS target #92 (MMSI: 992365362), which was decoded and displayed only twice. Additionally, both of the above AIS targets could not be verified, because there was no record of the existence of their MMSI numbers. Namely, every base/coast station, ship station or the AIS AtoN which

has been notified to the ITU Radiocommunication Bureau can be retrieved using ITU's Maritime mobile Access and Retrieval System (MARS) [32].

After eliminating incorrectly decoded and displayed AIS targets, the next step was to calculate the great circle distance (in nautical miles) between the SDR AIS receiver antenna and every position decoded from data packets using the following expression [33]:

$$d = 3440.065 \cos^{-1}[\sin \varphi_A \cdot \sin \cdot_B + \cos \varphi_A \cdot \cos \varphi_B \cdot \cos(\lambda_A - \lambda_B)] \text{ NM} \quad (1)$$

where (φ_A, λ_A) and (φ_B, λ_B) are position coordinates.

This was done to determine the line-of-sight and over-the-horizon radio waves propagation distances. The line-of-sight propagation distances (in nautical miles) in the conditions of the standard atmosphere can be calculated using the following expression [34]:

$$D \cong 2.23\left(\sqrt{h_t(m)} + \sqrt{h_r(m)}\right) \text{ NM} \quad (2)$$

where $h_t(m)$ and $h_r(m)$ are heights (in meters) of the transmitting and the receiving antenna, respectively. Given that the height of the SDR AIS receiver antenna is 32 m, in order to achieve the line-of-sight propagation in the conditions of the standard atmosphere at distance of, for example, 30 NM, the height of the transmitting antenna must be 61 m.

In addition, the calculated great circle distances were also used in order to calculate the Free Space Propagation Loss (FSPL) in dB, according to the following expression [35]:

$$20 \log_{10} \frac{4\pi d(m)}{\lambda(m)} = 20 \log_{10} d(m) + 20 \log_{10} f(MHz) - 27.56 \quad (3)$$

where $d(m)$, $\lambda(m)$ and $f(MHz)$ are distance (in meters), wavelength of the radio waves (in meters) and the frequency of the radio waves (in MHz), respectively.

After determining great circle distances, the AIS targets with greatest distances from the antenna of the SDR AIS receiver were analysed. Thus, AIS packets from the target #48 (MMSI: 992476138, Italian virtual AIS AtoN) have been received and successfully decoded 94 times (on average every 15 min). According to its decoded position (which was the same in all decoded AIS packets), the distance between the SDR AIS receiver antenna and this target was 471 NM (Figure 3).

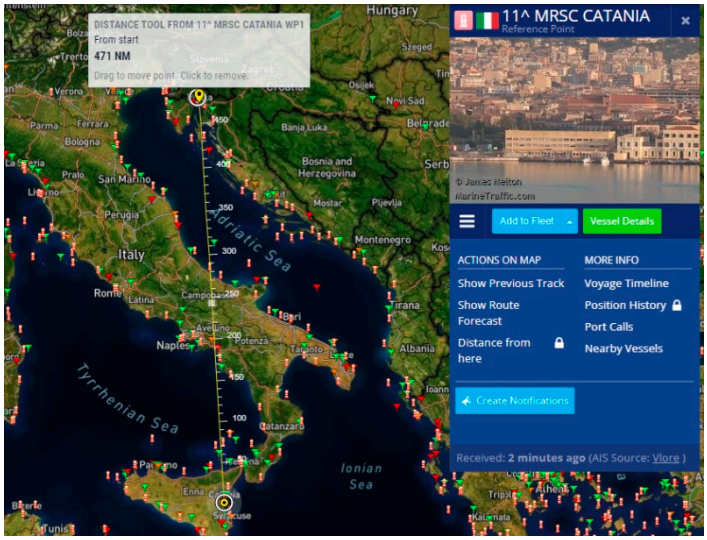

Figure 3. AIS target #48 [31].

This was considered as an over-the-horizon propagation. Otherwise, its antenna height must have been at 42,260 m! The FSPL from this target to the SDR AIS receiver

antenna was 135.44 dB. At the website of the NESDR SMArt v5 manufacturer there is no information on noise figure nor the receiver sensitivity, so these parameters are omitted in analysing the received power [28]. In the calculations of this research, the following was assumed:

AIS AtoNs transmit packets with 12.5 W power (the maximum power of any AIS station), which is 41 dBm;

There are no losses nor gains in both the transmitter (AtoN) and the receiver (antenna, coaxial cable and connectors/adapters, SDR and computer).

Thus, according to Friis transmission equation [36]:

$$P_r\ [\text{dBm}] = P_t\ [\text{dBm}] - \text{FSPL} \quad (4)$$

(where P_r [dBm] and P_t [dBm] are the received and transmitted power expressed in dBm), the received power from this target, which is the furthest detected at the SDR AIS receiver, was −94.44 dBm. According to [11], the typical AIS receiver should have the sensitivity around 20% PER @ −107 dBm, making this calculated value of the received power acceptable, since the SDR AIS receiver had 54.3% PER (bearing in mind that it is a low-cost device).

However, it must be emphasized that virtual AtoN messages, such as this target, are sent via AIS base stations, not necessarily limited only to local areas. Moreover, the same virtual AtoN message can be regularly broadcasted from several AIS base stations in order to ensure its redundancy [37].

The same observations apply for other Italian virtual AtoNs (MMSI: 992476xxx and 002470010) listed in Table 1.

Table 1. List of Italian virtual AtoNs (verified on [31]).

Target #	MMSI	Number of Decoded AIS Packets	Distance from the SDR AIS Receiver Antenna	Required Antenna Height for Line-of-Sight	Free Space Propagation Loss
48	992476138	94	471.0 NM	42,260 m	135.44 dB
54	992476140	79	436.9 NM	36,200 m	134.79 dB
64	992476139	89	435.3 NM	35,927 m	134.76 dB
18	992476141	98	341.3 NM	21,725 m	132.65 dB
22	992476132	104	273.6 NM	13,697 m	130.73 dB
32	992476130	105	269.5 NM	13,270 m	130.59 dB
60	992476127	106	241.0 NM	10,489 m	129.62 dB
51	002470010	100	226.7 NM	9216 m	129.09 dB
33	992476128	110	206.9 NM	7590 m	128.30 dB
31	992476133	116	172.4 NM	5134 m	126.71 dB
38	992476134	97	110.0 NM	1907 m	122.81 dB
65	992476135	106	104.5 NM	1698 m	122.37 dB
8	992476136	123	89.7 NM	1195 m	121.04 dB
50	992476137	123	34.1 NM	93 m	112.64 dB

Investigating [31], the nearest Italian AIS base station is Trieste (with elevation height of 50 m), which is 32 NM away from our antenna (Figure 4). It can be concluded that it is just a little bit over-the-horizon propagation (line-of-sight distance is 28.4 NM), therefore all Italian virtual AIS AtoNs could have been transmitted from this base station.

Furthermore, interesting observation can be made analysing AIS target #85 (MMSI: 992471104, Italian synthetic AtoN), from which only 2 AIS packets were received and successfully decoded. These packets were received on 25 February at 19:03 h and 19:40 h. As it can be seen from the Figure 5, this target is distant 190.1 NM from the receiver antenna.

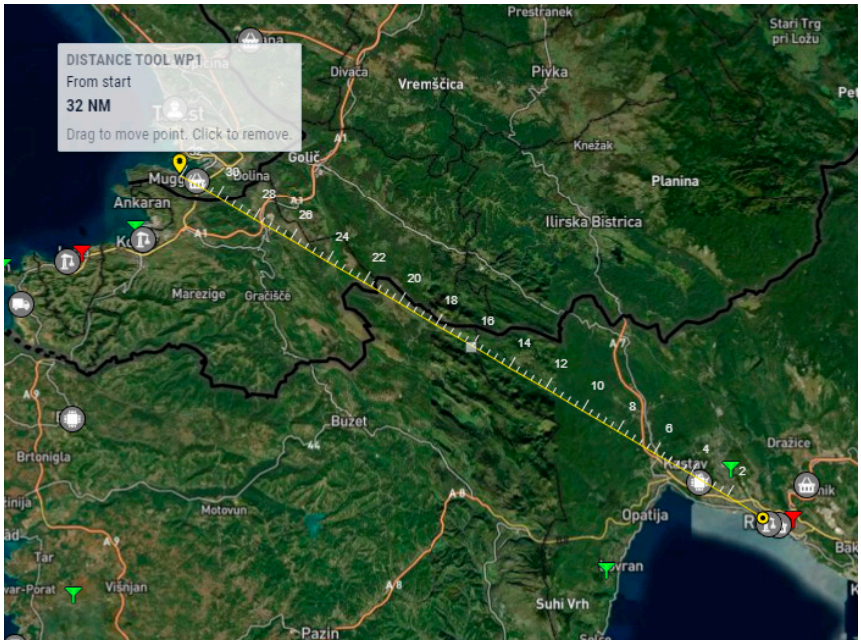

Figure 4. AIS base station Trieste [31].

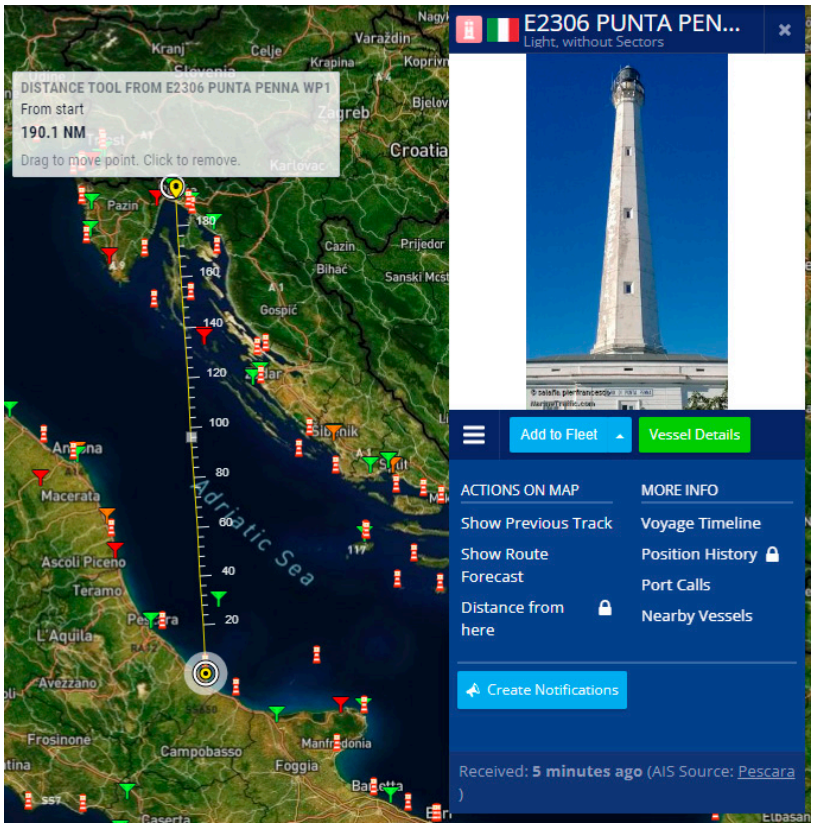

Figure 5. AIS target #85 [31].

Since this is a synthetic and not virtual AtoN, and only 2 AIS packets were decoded, this could be the actual radio signal range. Clearly, this is over-the-horizon propagation. The free space propagation loss from this target to the SDR AIS receiver antenna is 127.56 dB. This observation can also be applied on other Italian, as well as Croatian, synthetic and real AtoNs listed in Table 2.

Table 2. List of Italian and Croatian synthetic and real AtoNs (verified on [31]).

MMSI	Type of AtoN	Number of Decoded AIS Packets	Distance from PFRI Antenna	Required Antenna Height for Line-of-Sight	Free Space Propagation Loss
992471104	Synthetic	2	190.1 NM	6335 m	127.56 dB
992471105	Synthetic	4	178.4 NM	5527 m	127.01 dB
992471107	Synthetic	4	136.8 NM	3101 m	124.70 dB
992471109	Synthetic	79	110.0 NM	1907 m	122.81 dB
992471113	Synthetic	73	109.6 NM	1891 m	122.78 dB
992471112	Synthetic	87	108.9 NM	1864 m	122.72 dB
992471110	Synthetic	85	107.6 NM	1814 m	122.62 dB
992471162	N/A	4	95.5 NM	1381 m	121.58 dB
992381550	Real	4	78.9 NM	884 m	119.92 dB
992381330	Real	189	73.8 NM	753 m	119.34 dB
992381560	Real	9	73.2 NM	738 m	119.27 dB
992381060	Real	124	72.6 NM	724 m	119.20 dB
992381200	Real	684	66.6 NM	586 m	118.45 dB
992381340	Real	289	60.9 NM	469 m	117.68 dB
992381010	Real	166	55.6 NM	372 m	116.88 dB
992381190	Real	2919	49.3 NM	271 m	115.84 dB
992381260	Real	2227	43.5 NM	192 m	114.75 dB
992381100	Real	816	41.4 NM	167 m	114.32 dB
992383050	N/A	253	40.2 NM	153 m	114.07 dB
992381300	Real	1044	39.3 NM	143 m	113.87 dB
992381170	Real	2	39.3 NM	143 m	113.87 dB
992381110	Real	259	38.8 NM	138 m	113.76 dB
992381480	Real	5	38.3 NM	133 m	113.65 dB
992381220	Real	337	38.2 NM	132 m	113.62 dB
992381040	Real	961	37.8 NM	128 m	113.53 dB
992381320	Real	3700	28.0 NM	48 m	110.93 dB
992381310	Real	3516	25.6 NM	34 m	110.15 dB
992381120	Real	1356	25.3 NM	32 m	110.05 dB
992381430	Real	768	21.0 NM	14 m	108.43 dB

The mobile shipborne AIS stations (both Class A and B) were omitted in this analysis, because during the mentioned period of 24-h their AIS packets were received scarcely. Other AIS stations (base and AtoNs) from which AIS packets were received and decoded were within the line-of-sight range.

It remains to be answered why the over-the-horizon propagation of VHF/AIS radio waves appeared. As already mentioned, the conditions for detected anomalous propagation of AIS signals could be diffraction, tropospheric scattering, ionospheric sporadic E layer or refraction (subrefraction, superrefraction, ducting) [22,25–27].

However, according to [38] the diffraction effect can be neglected, since the wavelength of the AIS frequency is too short (app. 2 m) compared to the Earth's radius (app. 6371 km). Furthermore, according to the same reference, since the tropospheric scattering is primarily related to microwaves, this effect was also neglected during the analysis. Lastly, considering that in this research the reception of the AIS signals took place during the winter (February 2023), and ionospheric sporadic E layers occur mostly during the summer, this propagation mechanisms can also be neglected [22].

Therefore, deducing all the above, it can be concluded that the over-the-horizon propagation of AIS signals received by the SDR AIS receiver occurred due to the refraction effects.

In 2013, a scientific research conducted over the period of 15 years was published, in which statistical characteristics of the anomalous refractive conditions along the coast of the Adriatic Sea were determined [39]. On the basis of collected data from 4 Adriatic aerological stations, one group of the indicators that was determined and presented are the annual cycles of monthly percentages of occurrence of each of the possible refractive phenomena, i.e., subrefraction, superrefraction and ducting. Analysing these indicators, it

was evident that the largest number of anomalous propagation conditions occurred during summer months. However, the appearance of the phenomenon of superrefraction shows an increasing trend precisely at the end of February and at the beginning of March. In addition, from one of the stations, the percentage of occurrence of superrefraction at the end of February and at the beginning of March has almost the same values as during the summer months.

Following the above methodology, with the aim of proving refractive anomalous propagation, available data recorded by radiosondes from 9 stations located in Croatia (2) and Italy (7) were collected and used in this paper (Table 3). Each station records data up to twice a day (00:00 h and 12:00 h). These datasets were collected in the FAA604 (WMO/GTS) format from the database of the National Oceanic and Atmospheric Administration (NOAA) Earth System Research Laboratories (ESRL) and University of Wyoming for the period from 25 February 2023 at 00:00 UTC to 27 February 2023 at 00:00 UTC [40,41].

Table 3. List of WMO stations with radiosondes.

Station	WMO Number	Location	Elevation
Zagreb/Maksimir	14240	45.82° N, 016.03° E	123 m
Zadar	14430	44.09° N, 015.35° E	84 m
Udine/Rivolto	16045	45.97° N, 013.05° E	52 m
Novara/Cameri	16064	45.52° N, 008.67° E	178 m
Cuneo—Levaldigi	16113	44.53° N, 007.62° E	386 m
San Pietro Capofiume	16144	44.65° N, 011.62° E	38 m
Pratica di Mare	16245	41.65° N, 012.43° E	12 m
Lecce	16332	40.22° N, 018.15° E	6 m
Trapani/Birgi	16429	37.92° N, 012.50° E	14 m

The downloaded radiosonde datasets were used as an input in the Advanced Refractive Effects Prediction System (AREPS) program, to create an atmospheric profile [42]. The obtained profiles of the atmosphere with refraction phenomena for each measurement of each individual station/radiosonde are shown in the Figures 6–13.

From Figure 6, it can be seen that at three stations (Zagreb/Maksimir, Zadar and Udine/Rivolto) the phenomenon of superrefraction was detected at heights above 2 km. In addition, at approximately 3.4 km above the Zagreb/Maksimir station (left), a phenomenon of subrefraction was also detected.

Furthermore, from Figure 7, it is evident that at the Udine/Rivolto and Novara/Cameri stations subrefraction was detected at heights above 5 km, while the next measurement from the Novara/Cameri station also detected superrefraction at three different heights (right). With a further measurement, superrefraction was again detected at around 4 km above the station Novara/Cameri (Figure 8 left).

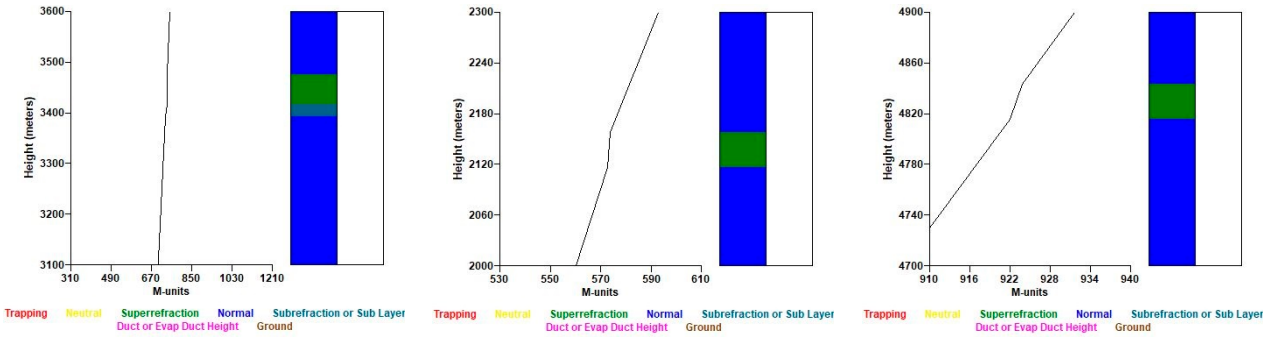

Figure 6. Zagreb/Maksimir, 25.2.2023, 12:00 UTC (**left**), Zadar, 25.2.2023, 00:00 UTC (**centre**), and Udine/Rivolto, 25.2.2023, 12:00 UTC (**right**).

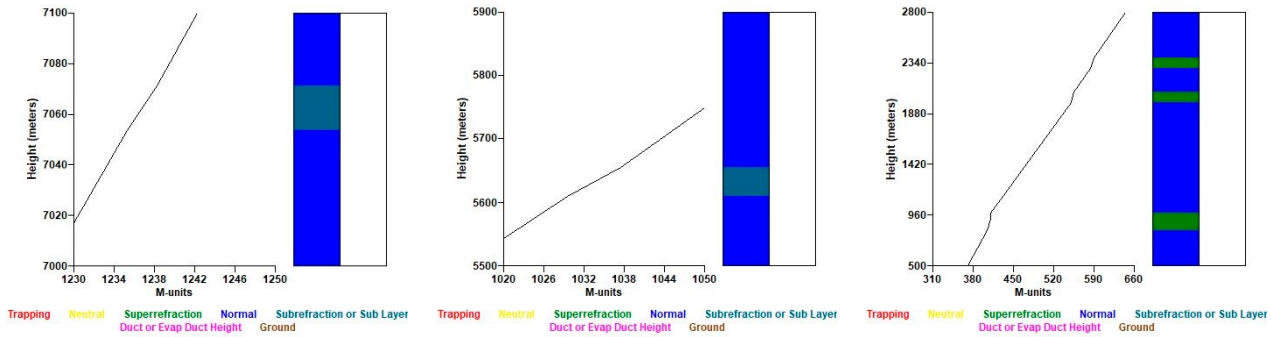

Figure 7. Udine/Rivolto, 26.2.2023, 12:00 UTC (**left**), Novara/Cameri, 25.2.2023, 00:00 UTC (**centre**), and Novara/Cameri, 26.2.2023, 00:00 UTC (**right**).

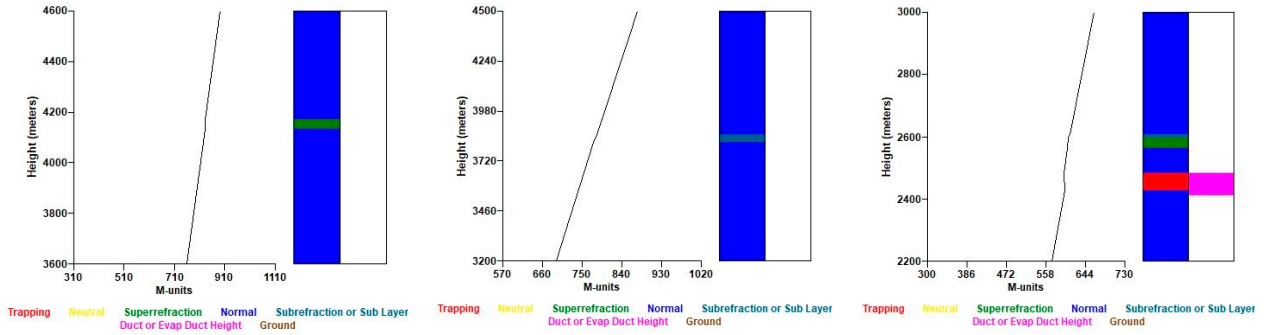

Figure 8. Novara/Cameri, 26.2.2023, 12:00 UTC (**left**), Cuneo—Levaldigi, 25.2.2023, 00:00 UTC (**centre**), and Cuneo—Levaldigi, 26.2.2023, 00:00 UTC (**right**).

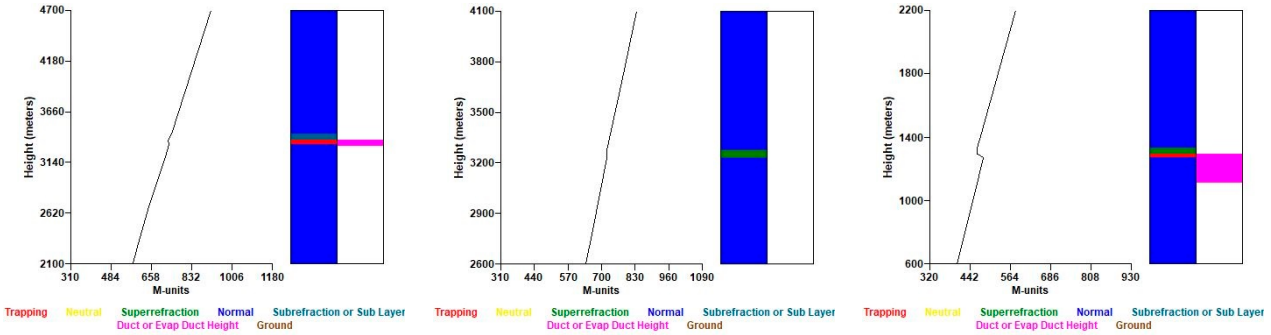

Figure 9. San Pietro Capofiume, 25.2.2023, 12:00 UTC (**left**), Pratica di Mare, 25.2.2023, 00:00 UTC (**centre**), and Pratica di Mare, 25.2.2023, 12:00 UTC (**right**).

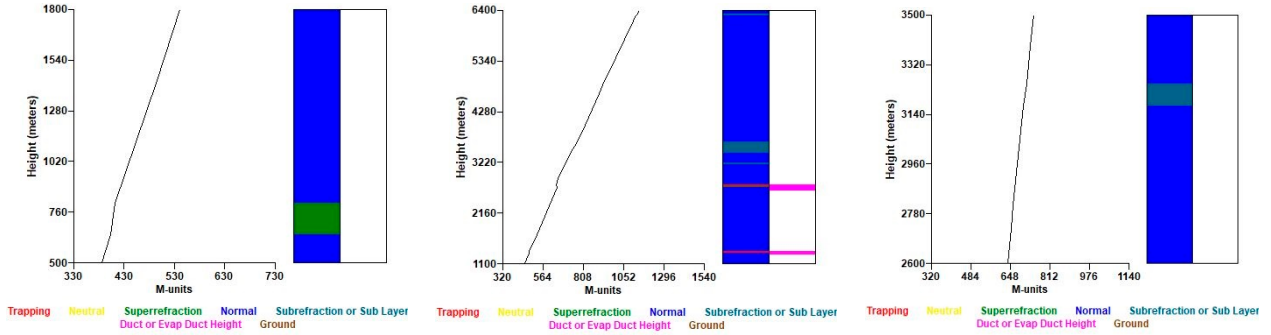

Figure 10. Pratica di Mare, 26.2.2023, 00:00 UTC (**left**), Pratica di Mare, 26.2.2023, 12:00 UTC (**centre**), Pratica di Mare, 27.2.2023, 00:00 UTC (**right**).

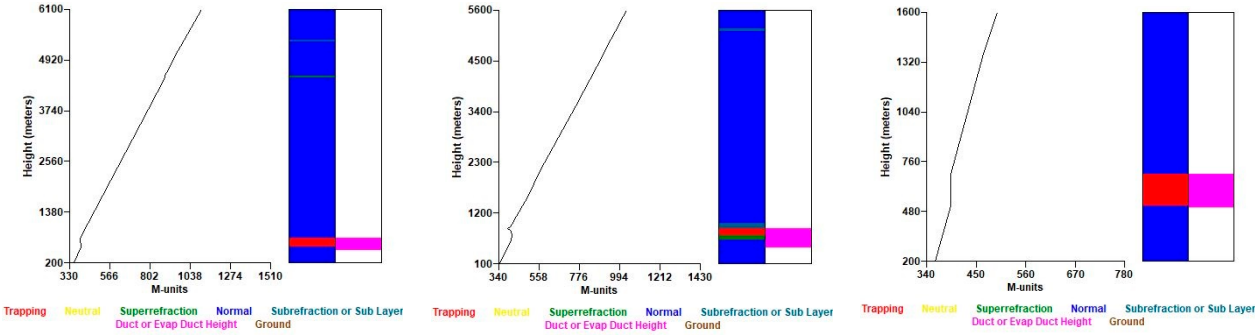

Figure 11. Lecce, 25.2.2023, 00:00 UTC (**left**), Lecce, 25.2.2023, 12:00 UTC (**centre**), Lecce, 26.2.2023, 00:00 UTC (**right**).

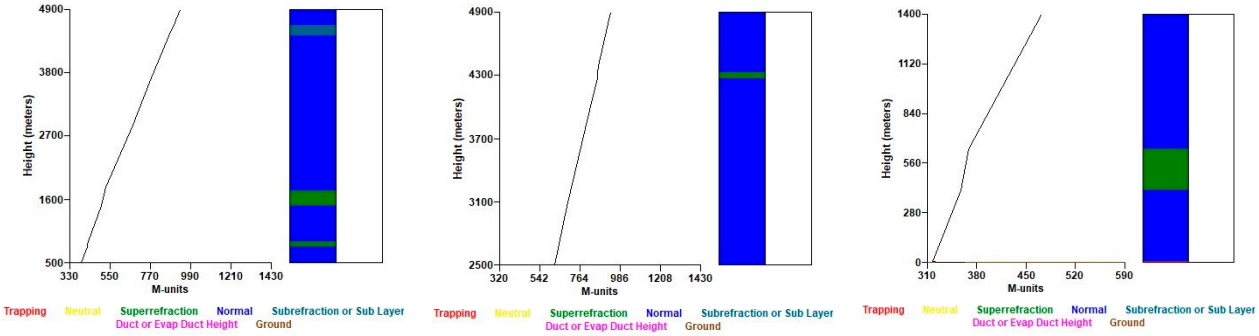

Figure 12. Lecce, 26.2.2023, 12:00 UTC (**left**), Trapani/Birgi, 25.2.2023, 00:00 UTC (**centre**), and Trapani/Birgi, 25.2.2023, 12:00 UTC (**right**).

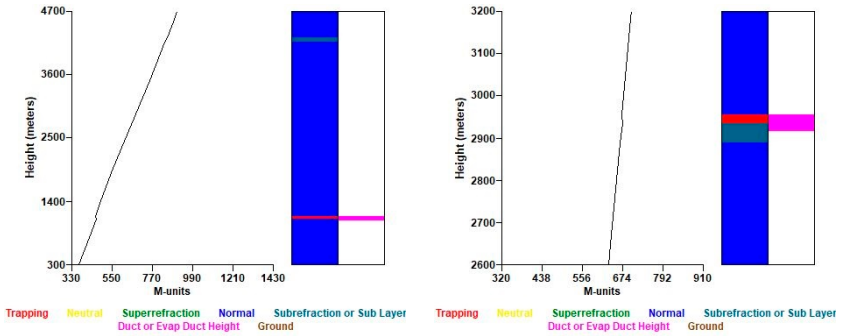

Figure 13. Trapani/Birgi, 26.2.2023, 00:00 UTC (**left**), and Trapani/Birgi, 26.2.2023, 12:00 UTC (**right**).

From Figure 8, it is also visible that at the station Cuneo—Levaldigi, during two different measurements, all refractive phenomena—subrefraction (centre), trapping/ducting and superrefraction (right) at heights above 2 km, were detected.

Analyzing Figure 9 left, it is evident that at the San Pietro Capofiume station, trapping/ducting and subrefraction effects were also detected at heights above 3 km. It can also be observed (centre and right) that during the first measurement above the Pratica di Mare station, superrefraction was detected at about 3.3 km, and during the second measurement trapping/ducting and superrefraction were detected at heights above 1 km.

Figure 10 shows three different measurements above the Pratica di Mare station. The first measurement (left) revealed superrefraction at a height around 750 m. Furthermore, the second measurement (centre) revealed trapping/ducting at two heights (about 1 km and about 3 km), as well as subrefraction (about 3.2 and 3.5 km), while during the third measurement (right), subrefraction was observed at a height above 3 km.

Moreover, in Figure 11, three different measurements above the Lecce station are shown. From the first measurement (left), all refractive phenomena were observed—

trapping/ducting at a height of 200 m and above, superrefraction at a height slightly below 5 km and subrefraction at a height above 5 km. The same observation can be seen from the next measurement (centre), but at much lower altitudes (between 200 m and 1200 m). From the third measurement (right), the phenomenon of trapping/ducting was observed at heights above 500 m.

Figure 12 shows one measurement from the Lecce station (left), and two measurements from the Trapani/Birgi station (centre and right). From the first measurement the superrefraction was detected at two different heights (above 500 m and above 1500 m), while the subrefraction was also detected at a height above 4 km. From the second and third measurements, the superrefraction was detected at heights above 4 km and above 500 m, respectively.

During both measurements over the Trapani/Birgi station (Figure 13), the same phenomena were observed—trapping/ducting and subrefraction, but at different heights.

As can be seen in the previous Figures, each station/radiosonde recorded the occurrence of refractive conditions in the atmosphere during the observed period within which the AIS signals were received. A summary of the detected refractive phenomena from the atmospheric profiles created by the AREPS program is shown in Table 4.

Table 4. Summary of the detected refractive phenomena by the AREPS program.

Station	Date and Time (UTC)	Refraction Type		
		Super-Refraction	Sub-Refraction	Ducting
Zagreb	25 February 2023, 12:00	X	X	
Zadar	25 February 2023, 00:00	X		
Udine	25 February 2023, 12:00	X		
	26 February 2023, 12:00		X	
Novara	25 February 2023, 00:00		X	
	26 February 2023, 00:00	X		
	26 February 2023, 12:00	X		
Cuneo	25 February 2023, 00:00		X	
	26 February 2023, 00:00	X		X
San Pietro	25 February 2023, 12:00		X	X
Pratica di Mare	25 February 2023, 00:00	X		
	25 February 2023, 12:00	X		X
	26 February 2023, 00:00	X		
	26 February 2023, 12:00		X	X
	27 February 2023, 00:00		X	
Lecce	25 February 2023, 00:00		X	X
	25 February 2023, 12:00	X	X	X
	26 February 2023, 00:00			X
	26 February 2023, 12:00	X	X	
Trapani	25 February 2023, 00:00	X		
	25 February 2023, 12:00	X		
	26 February 2023, 00:00		X	X
	26 February 2023, 12:00		X	X

To summarize, the presented results and findings provide a solid foundation for further research in the area of propagation of VHF radio waves and their anomalous features caused by the atmospheric effects. This paper presents a novel approach, i.e.,

the usage of a low-cost SDR AIS receiver specifically for this purpose—the detection of anomalous propagation conditions in the atmosphere above the Adriatic Sea region. Given that the most common form of maritime communication between navigators is a VHF radio station, this research, as well as future research on the same topic, can provide a further understanding towards VHF radio waves' propagation patterns and regularities in this region and beyond. In addition, if a new potential maritime system, being the VHF Data Exchange System (VDES) is used through the concept of e-navigation, these and future findings can be very useful from the point of view of automatic data exchange between (autonomous) vessels and terrestrial networks, as well as of remote monitoring of (autonomous) vessels.

The research results are applicable both in terms of the SDR assessment and prediction of VHF anomalous propagation caused by the refractive effects. These preliminary results will be the basis for the future research during different (seasons) and longer time periods, as well as at different locations.

Author Contributions: Both authors contributed to the manuscript equally. S.V.: Data collection and written; D.B.: Data collection and written. All authors have read and agreed to the published version of the manuscript.

Funding: This research received no external funding.

Institutional Review Board Statement: Not applicable.

Informed Consent Statement: Not applicable.

Data Availability Statement: Not applicable.

Acknowledgments: The authors would like to thank Mladen Viher, for generously providing access to the AREPS program, as well as detailed instructions for its use. This work has also been partially supported by MarineTraffic, which authorises the reproduction of live map images for the digital and printed formats of academic publications.

Conflicts of Interest: The authors declare no conflict of interest.

Appendix A

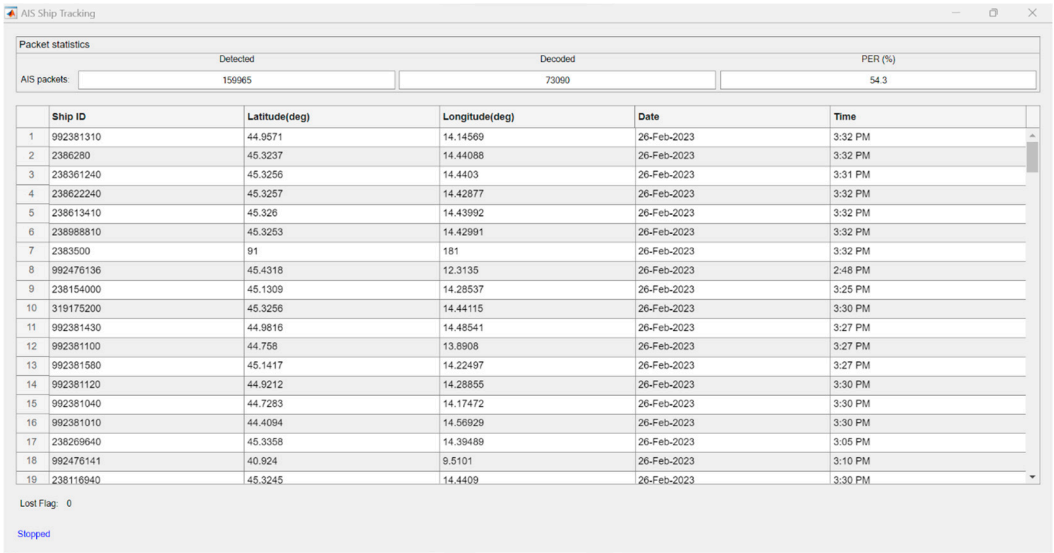

	Ship ID	Latitude(deg)	Longitude(deg)	Date	Time
1	992381310	44.9571	14.14569	26-Feb-2023	3:32 PM
2	2386280	45.3237	14.44088	26-Feb-2023	3:32 PM
3	238361240	45.3256	14.4403	26-Feb-2023	3:31 PM
4	238622240	45.3257	14.42877	26-Feb-2023	3:32 PM
5	238613410	45.326	14.43992	26-Feb-2023	3:32 PM
6	238988810	45.3253	14.42991	26-Feb-2023	3:32 PM
7	2383500	91	181	26-Feb-2023	3:32 PM
8	992476136	45.4318	12.3135	26-Feb-2023	2:48 PM
9	238154000	45.1309	14.28537	26-Feb-2023	3:25 PM
10	319175200	45.3256	14.44115	26-Feb-2023	3:30 PM
11	992381430	44.9816	14.48541	26-Feb-2023	3:27 PM
12	992381100	44.758	13.8908	26-Feb-2023	3:27 PM
13	992381580	45.1417	14.22497	26-Feb-2023	3:27 PM
14	992381120	44.9212	14.28855	26-Feb-2023	3:30 PM
15	992381040	44.7283	14.17472	26-Feb-2023	3:30 PM
16	992381010	44.4094	14.56929	26-Feb-2023	3:30 PM
17	238269640	45.3358	14.39489	26-Feb-2023	3:05 PM
18	992476141	40.924	9.5101	26-Feb-2023	3:10 PM
19	238116940	45.3245	14.4409	26-Feb-2023	3:30 PM

Figure A1. *Cont.*

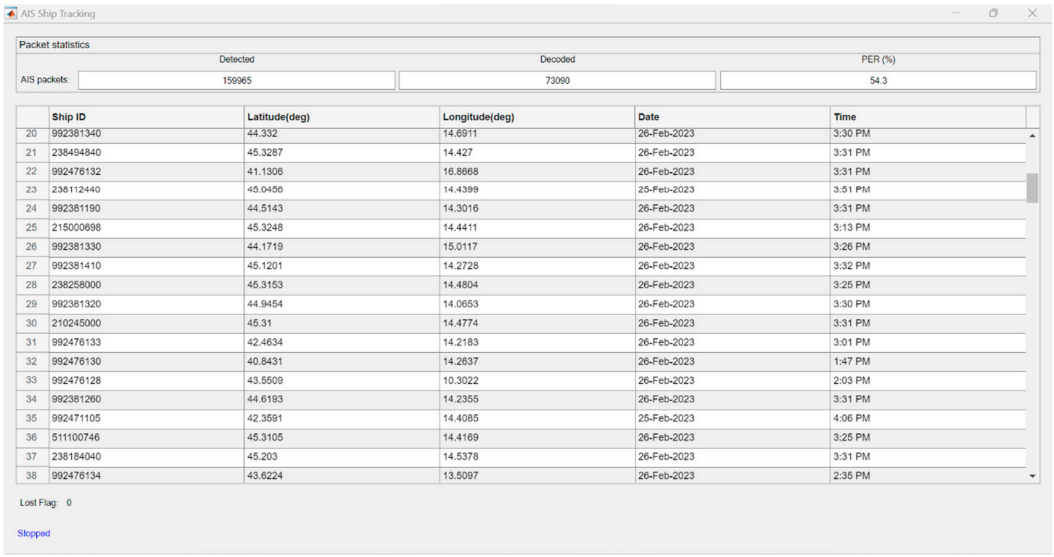

Figure A1. Decoded AIS targets #1 to #38.

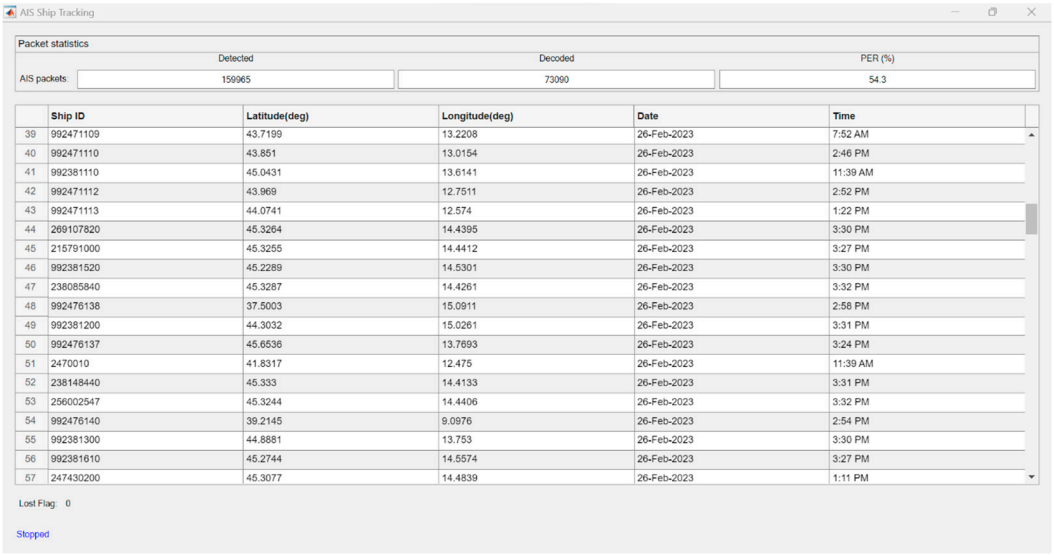

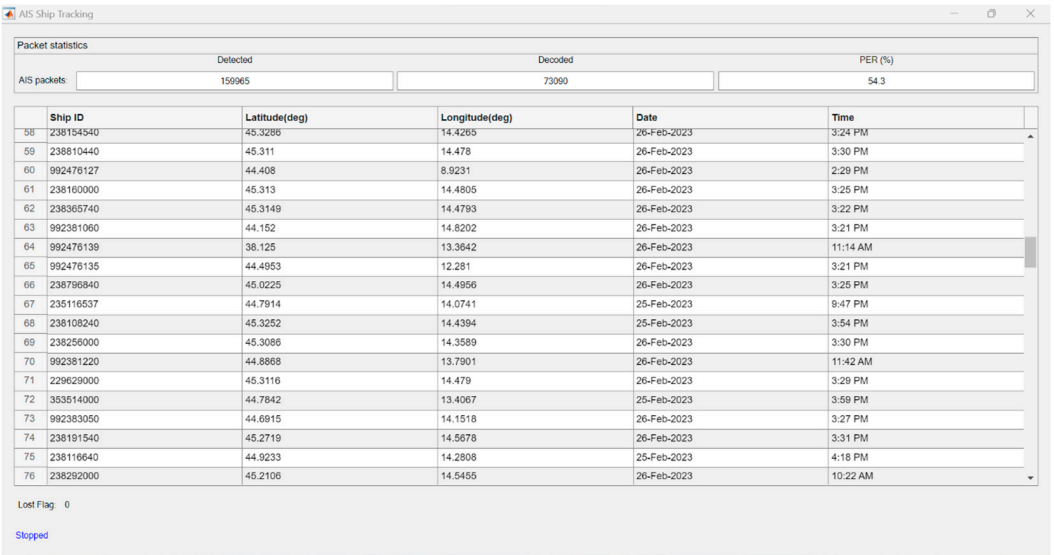

Figure A2. Decoded AIS targets #39 to #76.

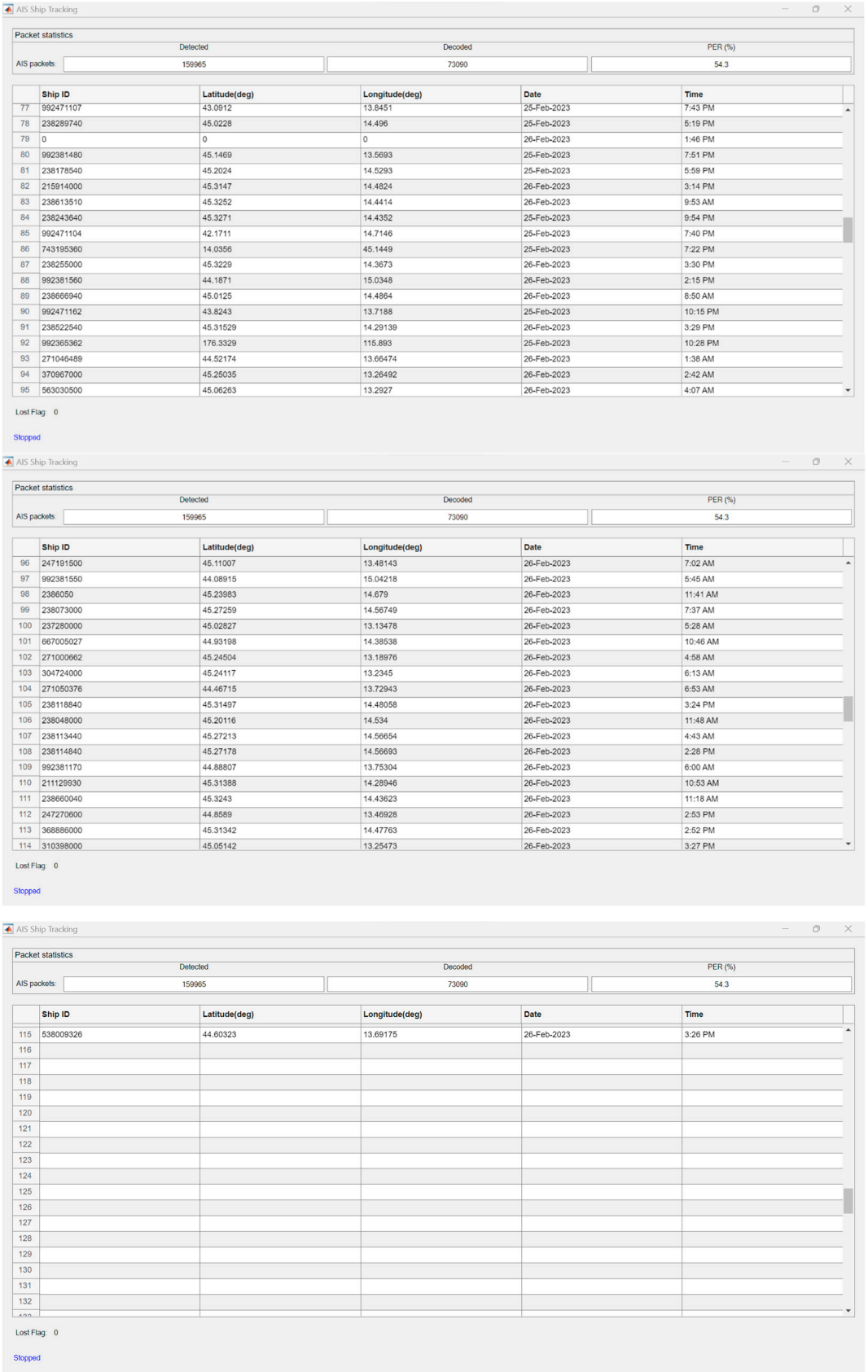

Figure A3. Decoded AIS targets #77 to #115.

References

1. International Telecommunication Union. *Recommendation ITU-R M.1371-5: Technical Characteristics for an Automatic Identification System Using Time Division Multiple Access in the VHF Maritime Mobile Frequency Band*; Electronic Publication: Geneva, Switzerland, 2014.
2. Ann, U.; Kügler, D.; Rohling, H. Analysis of Self-Organising Radio Systems for Position Reporting. *J. Navig.* **1999**, *52*, 196–202. [CrossRef]
3. Harre, I. AIS Adding New Quality to VTS Systems. *J. Navig.* **2000**, *53*, 527–539. [CrossRef]
4. Creech, J.; Ryan, J. AIS The Cornerstone of National Security? *J. Navig.* **2003**, *56*, 31–44. [CrossRef]
5. Mou, J.M.; van der Tak, C.; Ligteringen, H. Study on collision avoidance in busy waterways by using AIS data. *Ocean Eng.* **2010**, *37*, 483–490. [CrossRef]
6. Felski, A.; Jaskólski, K. Information unfitness as a factor constraining Automatic Identification System (AIS) application to anti-collision manoeuvring. *Pol. Marit. Res.* **2012**, *19*, 60–64. [CrossRef]
7. Pallotta, G.; Vespe, M.; Bryan, K. Vessel Pattern Knowledge Discovery from AIS Data: A Framework for Anomaly Detection and Route Prediction. *Entropy* **2013**, *15*, 2218–2245. [CrossRef]
8. Tu, E.; Zhang, G.; Rachmawati, L.; Rajabally, E.; Huang, G.-B. Exploiting AIS Data for Intelligent Maritime Navigation: A Comprehensive Survey from Data to Methodology. *IEEE Trans. Intell. Transp. Syst.* **2018**, *19*, 1559–1582. [CrossRef]
9. Yang, D.; Wu, L.; Wang, S.; Jia, H.; Li, K.X. How big data enriches maritime research—A critical review of Automatic Identification System (AIS) data applications. *Transp. Rev.* **2019**, *39*, 755–773. [CrossRef]
10. Svanberg, M.; Santen, V.; Horteborn, A.; Holm, H.; Finnsgard, C. AIS in maritime research. *Mar. Policy* **2019**, *106*, 103520. [CrossRef]
11. Lang, H.; Wu, S.; Xu, Y. Ship Classification in SAR Images Improved by AIS Knowledge Transfer. *IEEE Geosci. Remote Sens. Lett.* **2018**, *15*, 439–443. [CrossRef]
12. Prust, C. Introductory Communication Systems Course Using SDR. MATLAB Central File Exchange. Available online: https://www.mathworks.com/matlabcentral/fileexchange/69417-introductory-communication-systems-course-using-sdr (accessed on 17 March 2023).
13. Stewart, R.W.; Barlee, K.W.; Atkinson, D.S.W.; Crockett, L.H. *Software Defined Radio Using MATLAB & Simulink and the RTL-SDR*; Strathclyde Academic Media: Glasgow, UK, 2017.
14. Cabrera, F.; Molina, N.; Tichavska, M.; Araña, V. Automatic Identification System modular receiver for academic purposes. *Radio Sci.* **2016**, *51*, 1038–1047. [CrossRef]
15. Mathapo, K.F. A Software-Defined Radio Implementation of Maritime AIS. Master's Thesis, University of Stellenbosch, Stellenbosch, South Africa, 2007.
16. Romero-Godoy, D.; Molina-Padrón, N.; Cabrera, F.; Araña, V.; Jiménez, E. Design and implementation of a prototype with a low-cost SDR platform for the next generation of maritime communications. In Proceedings of the 2022 3rd URSI Atlantic and Asia Pacific Radio Science Meeting (AT-AP-RASC), Gran Canaria, Spain, 30 May–4 June 2022; pp. 1–4. [CrossRef]
17. Budroweit, J. Software-defined radio with flexible RF front end for satellite maritime radio applications. *CEAS Space J.* **2013**, *8*, 201–213. [CrossRef]
18. Cruz, F.R.G.; Gania, R.C.M.; Garcia, B.W.C.; Nob, J.C.R. Software Defined Radio Implementation of a Single Channel Automatic Identification System Receiver. In Proceedings of the TENCON 2018–2018 IEEE Region 10 Conference, Jeju, Republic of Korea, 28–31 October 2018; pp. 2452–2455. [CrossRef]
19. Marques, M.M.; Teles, D.; Lobo, V.; Capela, G. Low-cost AIS Transponder using an SDR device. In Proceedings of the OCEANS 2019 MTS/IEEE SEATTLE, Seattle, WA, USA, 27–31 October 2019; pp. 1–4. [CrossRef]
20. Bažec, M.; Dimc, F. Decoding AIS Messages with the use of Low Performance Sofware Defined Radio. In Proceedings of the 13th Annual Baška GNSS Conference Proceedings, Baska, Croatia, 12–15 May 2019; pp. 77–85.
21. Ames, L.A.; Newman, P.; Rogers, T.F. VHF tropospheric overwater measurements far beyond the radio horizon. *Proc. IRE* **1955**, *43*, 1369–1373. [CrossRef]
22. Chartier, A.T.; Hanley, T.R.; Emmons, D.J. Long-distance propagation of 162 MHz shipping information links associated with sporadic E. *Atmos. Meas. Tech.* **2022**, *15*, 6387–6393. [CrossRef]
23. Tang, H.; Wang, H.; Jiao, L.; Li, Y. Analysis of Ultra-short Wave Propagation in Atmospheric Duct. In Proceedings of the 12th International Symposium on Antennas, Propagation and EM Theory (ISAPE), Hangzhou, China, 3–6 December 2018; pp. 1–4. [CrossRef]
24. Bruin, E.R. On Propagation Effects in Maritime Situation Awareness: Modelling the Impact of North Sea Weather Conditions on the Performance of AIS and Coastal Radar Systems. Master's Thesis, Utrecht University, Utrecht, The Netherlands, 2016.
25. Constantinides, A.; Najat, S.; Haralambous, H. Atmospheric Ducting Interference on DAB, DAB+ Radio in Eastern Mediterranean. *Electronics* **2022**, *11*, 4183. [CrossRef]
26. Lee, I.-S.; Noh, J.-H.; Oh, S.-J. A Survey and analysis on a troposcatter propagation model based on ITU-R recommendations. *ICT Express* **2022**, *in press*. [CrossRef]
27. Tang, W.; Cha, H.; Wei, M.; Tian, B. The effect of atmospheric ducts on the propagation of AIS signals. *Aust. J. Electr. Electron. Eng.* **2019**, *16*, 111–116. [CrossRef]

28. Nooelec. NESDR SMArt v5 SDR. Available online: https://www.nooelec.com/store/sdr/sdr-receivers/nesdr-smart-sdr.html (accessed on 3 April 2023).
29. MathWorks®. Ship Tracking Using AIS Signals. Available online: https://uk.mathworks.com/help/comm/ug/ship-tracking-using-ais-signals.html (accessed on 3 April 2023).
30. Scan-Antenna. VHF74 Datasheet. Available online: https://www.scan-antenna.com/umbraco/surface/product/GetProductForPDF?productId=5365 (accessed on 3 April 2023).
31. Marine Traffic—Global Ship Tracking Intelligence. Available online: https://www.marinetraffic.com (accessed on 3 April 2023).
32. International Telecommunication Union, Maritime mobile Access and Retrieval System (MARS). Available online: https://www.itu.int/en/ITU-R/terrestrial/mars/Pages/default.aspx (accessed on 3 April 2023).
33. Kells, L.M.; Kern, W.F.; Bland, J.R. *Plane and Spherical Trigonometry*; McGraw Hill Book Company, Inc.: New York, NY, USA, 1940.
34. Richards, J.A. *Radio Wave Propagation*; Springer: Berlin/Heidelberg, Germany, 2008.
35. Jagannatham, A.K. *Principles Of Modern Wireless Communications Systems*; McGraw Hill Education (India) Private Limited: New Delhi, India, 2016.
36. Balanis, C.A. *Antenna Theory*; Wiley-Interscience: New York, NY, USA, 2005.
37. International Association of Marine Aids to Navigation and Lighthouse Authorities (IALA) Guideline. In *G1081 Provision of Virtual Marine Aids to Navigation, 2.1 ed.*; IALA: Saint Germain en Laye, France, 2021.
38. Son, H.K.; Lee, S.H. The Prediction of Radio Interference through Ducting and Proposal measures for Protecting Interference. In Proceedings of the Vehicular Technology Conference, IEEE 55th Vehicular Technology Conference, Birmingham, AL, USA, 6–9 May 2002.
39. Viher, M.; Telišman Prtenjak, M.; Grisogono, B. A multi-year study of the anomalous propagation conditions along the coast of the Adriatic Sea. *J. Atmos. Sol. Terr. Phys.* **2013**, *97*, 75–84. [CrossRef]
40. National Oceanic and Atmospheric Administration (NOAA) Earth System Research Laboratories (ESRL). NOAA/ESRL Radiosonde Database. Available online: https://ruc.noaa.gov/raobs (accessed on 3 April 2023).
41. University of Wyoming, College of Engineering, Department of Atmospheric Science. Available online: http://weather.uwyo.edu/upperair/sounding.html (accessed on 3 April 2023).
42. Barrios, A.E.; Patterson, W.L. *Advanced Propagation Model v.1.3.1 Computer Software Configuration Item (CSCI) Documents: Technical Document 3145*; SPAWAR Systems Center: San Diego, CA, USA, 2002.